Thermo-oxidative aging of epoxy coating systems

Y. Zahra [a,b], F. Djouani [a], B. Fayolle [a,*], M. Kuntz [b], J. Verdu [a]

[a] Laboratoire Procédé et Ingénierie en Mécanique et Matériaux (PIMM-UMR8006), Arts et Métiers ParisTech ENSAM, 151 Boulevard de l'Hôpital, 75013 Paris, France
[b] EDF R&D, Département Matériaux et Mécanique des Composants, Avenue des Renardières, Ecuelles, 77250 Moret sur Loing, France

A B S T R A C T

The thermo-oxidative behavior of unformulated (unfilled) samples of epoxy coatings has been studied at five temperatures ranging from 70 °C to 150 °C. Two epoxy networks based on diglycidyl ether of bisphenol A (DGEBA), respectively, cured by jeffamine (POPA) or polyamidoamine (PAA) were compared. Infrared spectrophotometry (IR), differential scanning (DSC) and sol–gel analysis (SGA) were used to monitor structural changes.

Thermal oxidation leads to carbonyl and amide formation in both systems. POPA systems appear more sensitive to oxidation than PAA ones. Thermal oxidation leads to predominant chain scission as evidenced by the decrease of glass transition temperatures (T_g) and increase of sol fraction.

Keywords:
Epoxy
Coating
Jeffamine
Polyamidoamine
Oxidation
Degradation

1. Introduction

Epoxy networks cured by aliphatic diamines are commonly used as coatings in nuclear industry where durability is a key property. Typical exposure conditions are a constant temperature of about 50 °C and 0.1 Gy h^{-1} of irradiation dose rate, in air.

In a study of polyethylene insulating materials exposed in these conditions, Khelidj et al. [1] proposed a kinetic approach which can be widely generalized. It is based on the graph of Fig. 1 in which the polymer lifetime is plotted against dose rate, both in logarithmic scales.

Three kinetic regimes can be distinguished as following: regime I in which radical initiation results almost exclusively from polymer radiolysis. This regime corresponds to a linear asymptote of slope unity in the simplest cases. Regime III, in which initiation by polymer radiolysis is negligible in front of initiation by hydroperoxide thermal decomposition. This regime corresponds to a horizontal asymptote of which the ordinate is the lifetime in thermal aging at the temperature under consideration.

Regime II is a transition phase between regime (I) and (III). In this regime, initiation by polymer radiolysis predominates at the beginning of exposure, it creates hydroperoxides which accumulate until the time where their concentration reaches a critical value. At this point, their thermal decomposition becomes the predominant radical source and the polymer undergoes a thermal aging process. Indeed the boundaries between these kinetic regimes sharply depend on different factors such as the radiochemical yield for radical formation (G_i), the stability of hydroperoxides, the occurrence of anaerobic radiochemical processes in the sample core, etc.

In a recent publication [2], we have reported results of an investigation aimed to explore essentially the regime (I) for both systems under study. Some peculiarities of POPA and PAA structures were put in evidence and it was shown that, for the dose rates of practical interest ($\leq$0.1 Gy h^{-1}), aging is dominated by thermal oxidation (regime III), that justifies this work.

There is some literature on thermal aging of epoxy networks [3–8] in a wide temperature range, using analytical tools such as DSC [9], ATG [10], DMTA, FTIR, UV [11] and XPS [12]. Some recurrent features of aging behavior are: the eventual occurrence of post-cure reactions coexisting with oxidation [13,14], carbonyl growth [15,16,10,17], and chain scission [18,19]. This latter process is especially important owing to its role in polymer embrittlement [20].

The aim of this article is to compare the thermal oxidative stability of POPA and PAA systems using free films.

2. Experimental part

2.1. Materials

The diglycidyl ether of bisphenol A (DGEBA) used in this study has an epoxide concentration of 1.71 mol kg^{-1} corresponding to

* Corresponding author. Tel.: +33 14424 6413; fax: +33 14424 6382.
E-mail addresses: bruno.fayolle@ensam.eu, bruno.fayolle@paris.ensam.fr (B. Fayolle).

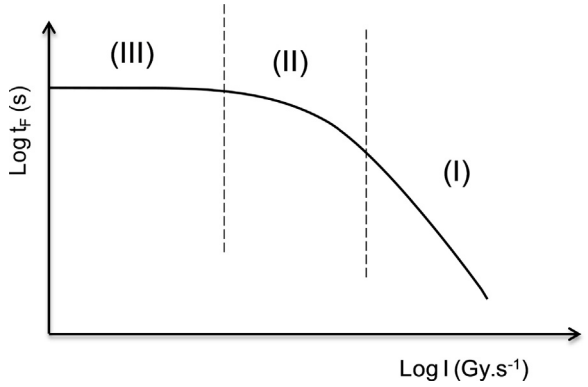

Fig. 1. General shape of the log (lifetime) – log (dose rate) curve at a given temperature.

a number average molar mass Mn = 1170 g mol^{-1} and a degree of polymerization n = 3.

The polyamidoamine (PAA) has a number average molar mass close to 1230 g mol^{-1} corresponding to a degree of polymerization j = 3.9.

The polyoxyproylene (POPA) has a number average molar mass 132 g mol^{-1} corresponding to a degree of polymerization x = 3.

The structure of these components is shown in Fig. 2.

Stoichiometric epoxide-amine mixtures were used to obtain films of 100–150 μm in thickness. These films were cured at room temperature (RT) for 3 days to be post-cured at 110 °C under vacuum later on for 48 h. The aim of the post curing is to reach a fully cured network structure as close as possible to the ideal one (only elastically active chains, no dangling chains).

They are transparent (no significant phase segregation) and slightly yellow (limited oxidation during processing).

2.2. Aging

Thermal aging was carried out in ventilated ovens under 70, 90, 110, 130 and 150 °C range of temperature. The films were regularly removed from ovens to be analyzed.

2.3. Characterization

FTIR spectrophotometry was performed in ATR mode with a Bruker IFS 28 spectrophotometer in the 4000–600 cm^{-1} spectral range, averaging 64 scans for a resolution of 4 cm^{-1}. A defined base line has been fixed for all FTIR spectra. Absorbance values are measured by the height of peak from the defined base line for a given wavenumber. Quantitative measurements were made using the following relationship:

$$[\text{Species}] = \frac{\varepsilon_{\text{Ar}}[\text{Ar}]}{\varepsilon_{\text{Species}}} \frac{\text{A(Species)}}{\text{A(Ar)}} \quad (1)$$

where A (species) and ε species are the absorbance and the molar absorptivity of the species, respectively. The peak at 1606 cm^{-1}, whose intensity is invariant throughout degradation, has been taken as reference. The carbonyl and amide concentration were determined by using the Beer–Lambert law in which molar absorptivity usual value of 500 L mol^{-1} cm^{-1} for carbonyl at 1730 cm^{-1} and 470 L mol^{-1} cm^{-1} for amide groups at 1658 cm^{-1} and 240 L mol^{-1} cm^{-1} for aromatic bands at 1606 cm^{-1} [21].

DSC measurements were carried out using a Q1000 modulated differential scanning calorimeter (TA instruments) in a nitrogen flow (50 ml min^{-1}). Samples weights were ranged between 5 and 10 mg. A temperature ramp of 2 °C min^{-1} was used from 0 to 170 °C. A temperature modulation of 0.318 °C with a period of 60 s was superimposed to the main signal to record simultaneously reversible and irreversible heat flows. T_g values were assessed from the reversible heat flow curve, since the reversible signal is associated to physical modifications.

The sol fraction in tetrahydrofurane (THF) was determined in soxhlet for 24 h. During thermal exposure, chain scissions occurring increase the soluble fraction by increasing the number of chains that are no longer related to the network. In order to assess sol fraction, samples have been weighted before and after extraction. Initial weight (m_i) of sample ranged from 70 to 100 mg. After 24 h of extraction, the samples were dried during 24 h at 70 °C and weighted (m_f). Soluble fraction (w_s) was calculated by the following equation:

$$w_s = \frac{m_i - m_f}{m_i} \quad (2)$$

3. Results and discussion

3.1. Amide formation

The most spectacular changes of IR spectrum occur in the 1630–1690 cm^{-1} interval (Fig. 3), and can be attributed to amide formation. For long exposure times, both systems display their

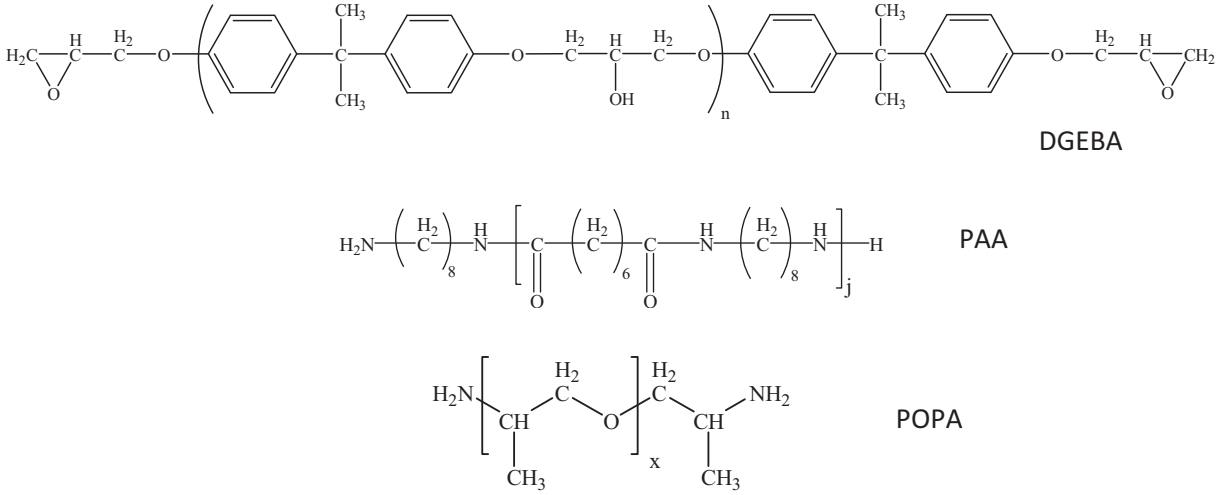

Fig. 2. Chemical structure of "monomers".

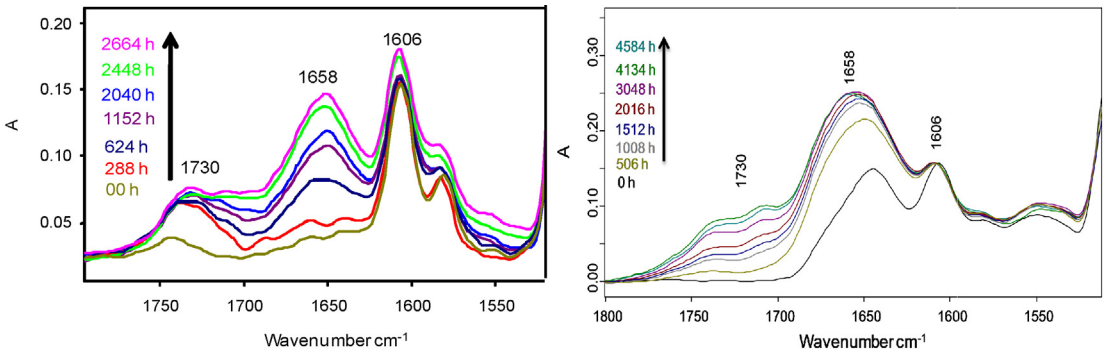

Fig. 3. FTIR spectra in the 1520–1800 cm^{-1} domain, left: POPA system, right: PAA system during exposure in air at 110 °C.

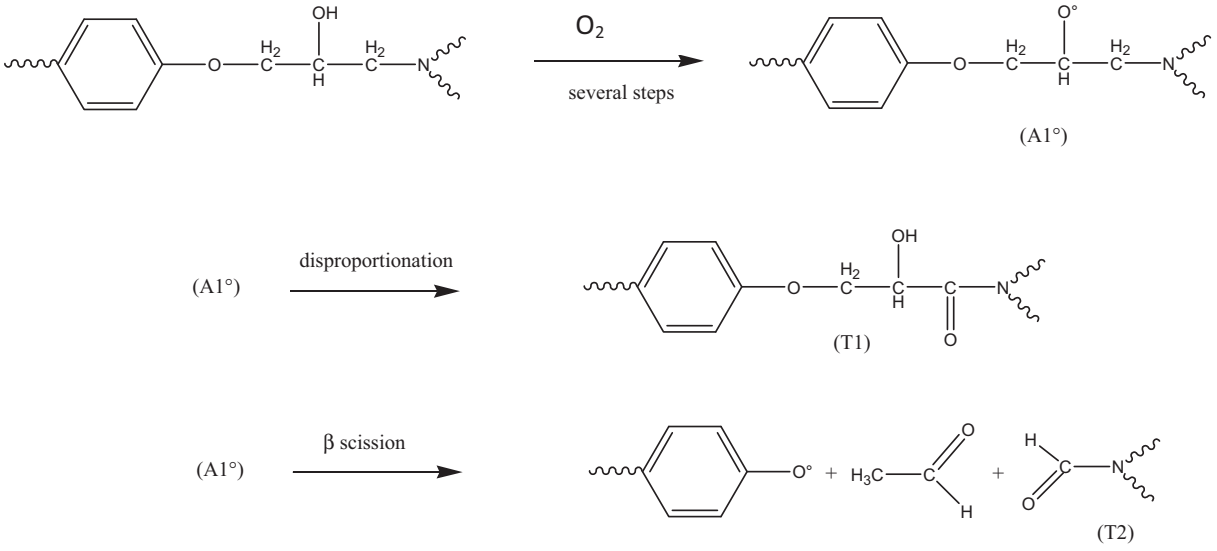

Fig. 4. Possible routes for the formation of tertiary amides, absorbing at 1658 cm^{-1}, common to both systems.

maximum absorption at 1658 cm^{-1}, suggesting that the same types of amides are formed in DGEBA/POPA and DGEBA/PAA. Amides result necessarily from the oxidative attack of α amino carbon. It can be thus deduced that the amide absorbing at 1658 cm^{-1} results from oxidation of the α amino carbon belonging to the DGEBA segments (Fig. 4).

At this state of our knowledge, we can envisage the formation of two types of amides: T1 and T2. The stability of T1 is unknown.

At short exposure times, clear difference can be observed between our two studied systems. In DGEBA/PAA, secondary amides belonging to PAA segments are initially present; they absorb at ca. 1645 cm^{-1}. The peak maximum shifts gradually

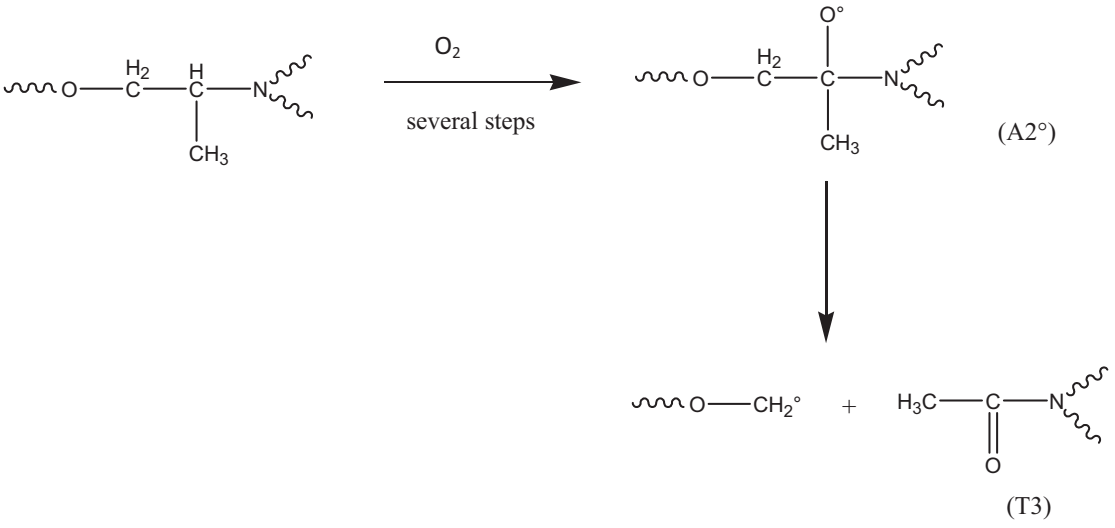

Fig. 5. Possible route for the formation of acetamide absorbing at 1665 cm^{-1}.

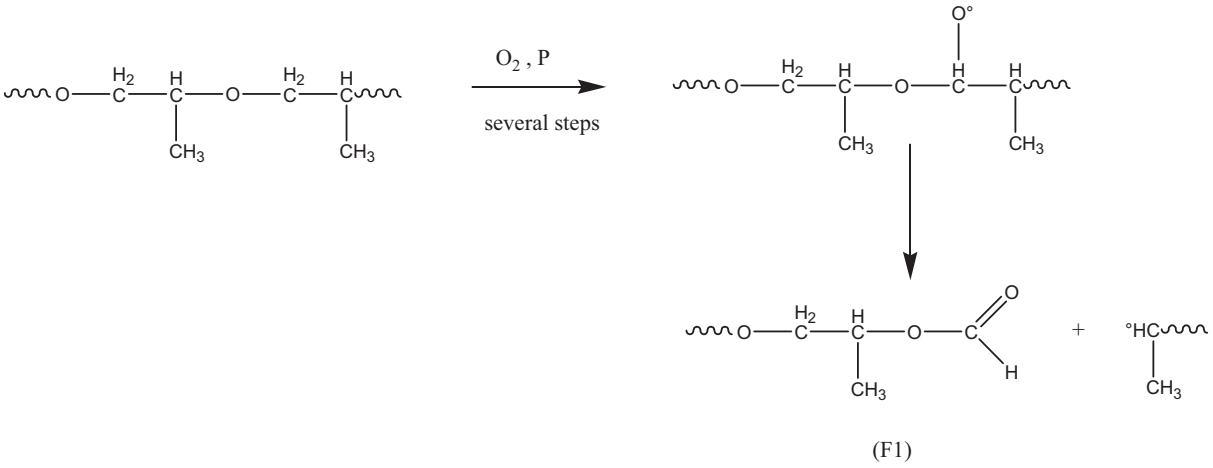

Fig. 6. Possible route for formate formation in POPA networks.

toward 1658 cm^{-1} during oxidation, no supplementary fine structure was observed, which can be interpreted as follow: in this system, only α amino carbons belonging to DGEBA segments are transformed into amides according to mechanisms shown in Fig. 4.

In DGEBA/POPA, where initially no amide is present, the spectral changes are completely different at short exposure times: a band appears first at ca. 1665 cm^{-1} and grows rapidly but reaches a pseudo asymptotic intensity after ca. 600 h. Then, the 1658 cm^{-1} band tends to become predominant. Logically, the band at 1665 cm^{-1} must correspond to an amide resulting from the oxidation of the α amino carbon belonging to POPA segment (Fig. 5). This process is expected to give an acetamide (T3) by β scission of the tertiary alkoxyl (A2°) precursor.

3.2. Carbonyl formation

Carbonyls, other than amide ones, absorb in the 1690–1790 cm^{-1} spectral range. FTIR spectra (Fig. 3) reveal the growth of a wide band with a complex fine structure showing the formation of a great diversity of carbonyl/carboxyl species. DGEBA/PAA and DGEBA/POPA differ significantly by the following features:

In DGEBA/POPA, the absorption in the 1720–1740 cm^{-1} interval increases abruptly in the first days of exposure. This absorption mainly results from the overlapping of two peaks: one located near to 1720 cm^{-1}, the other located near to 1740 cm^{-1}. At long term ($t > 288$ h), the intensity of both peaks remains almost constant whereas other carbonyl containing species absorbing between 1690 and 1720 cm^{-1} continue to grow. Absorbance changes above 1750 cm^{-1} are negligible.

In DGEBA/PAA, a completely different behavior is observed: two predominant species absorbing respectively at ca. 1715 and ca. 1745 cm^{-1} appear and grow progressively during the whole exposure duration. The absorbance above 1750 cm^{-1} increases significantly.

3.3. These changes call for the following comments

POPA segments are highly reactive toward oxidation owing to the low stability of the tertiary CH bond and the destabilizing effect of neighboring ether group. Polyoxypropylene was recognized one half century ago as one of the most oxidizable polymers [22].

In our previous study of radiation induced oxidation [2], we have put in evidence the formation of a methyl ketone (MK) absorbing at 1722 cm^{-1}.

MK is presumably responsible for one component of the doublet formed at short time ($t \leq 288$ h) in POPA spectra. The other component absorbing at ca. 1740 cm^{-1} was absent from the spectra of irradiated samples and can be presumably attributed to the thermal decomposition of a species stable at ambient temperature. The first hypothesis which comes in mind is, indeed, hydroperoxide decomposition, but this latter must lead to the same alkoxyl as in radiochemically initiated oxidation. In a first approach two routes can be envisaged.

At $T > 70$ °C, a part of peroxy radicals can abstract hydrogens on methylenes of which the oxidation could lead to formates (F1) absorbing close to 1740 cm^{-1} (Fig. 6).

Tertiary alkoxy radicals react preferentially at 20 °C by β scission on the C—O side to give a methyl ketone. But at high temperature, they have enough vibrational energy to break the C—C bond and to give acetate (C1, Fig. 7).

In PAA networks, where all the carbonyl species grow in the same timescale, it is difficult to distinguish between the ones formed in PAA segments and the ones formed in DGEBA segments, more precisely in isopropanol segments.

In PAA segments, the most reactive site is, no doubt, the α amido nitrogen [23] which is expected to give mainly imides and aldehydes (Fig. 8). Unfortunately, imides are difficult to distinguish from other carbonyl species absorbing between 1700–1750 cm^{-1}. Aldehydes are rapidly oxidized into peracids and acids. Oxidation of the isopropanol segment must give the same products in PAA and POPA systems but in these latter, their IR absorption would be masked by the one coming from the oxidation of POPA segments.

It is interesting to notice that most of the process proposed in Figs. 4–8 lead to chain scissions with the exception of processes leading to T1 (Fig. 4) and I1 (Fig. 8).

3.4. Kinetic aspects

Carbonyl and amides build-up curves display strongly autoretarded character in both systems. Examples of curves are given, for the exposure at 110 °C, in Fig. 9. Initial rate values are given in Table 1.

3.5. These results call for the following comments

Initial rates of carbonyl and amides build-up are always in the same order of magnitude in POPA and PAA networks. Amides build-up is faster than carbonyl build-up at all temperatures in PAA networks. It is faster at high temperatures (≥150 °C) and slower at low temperatures (≤90 °C) for POPA networks. Activation energies

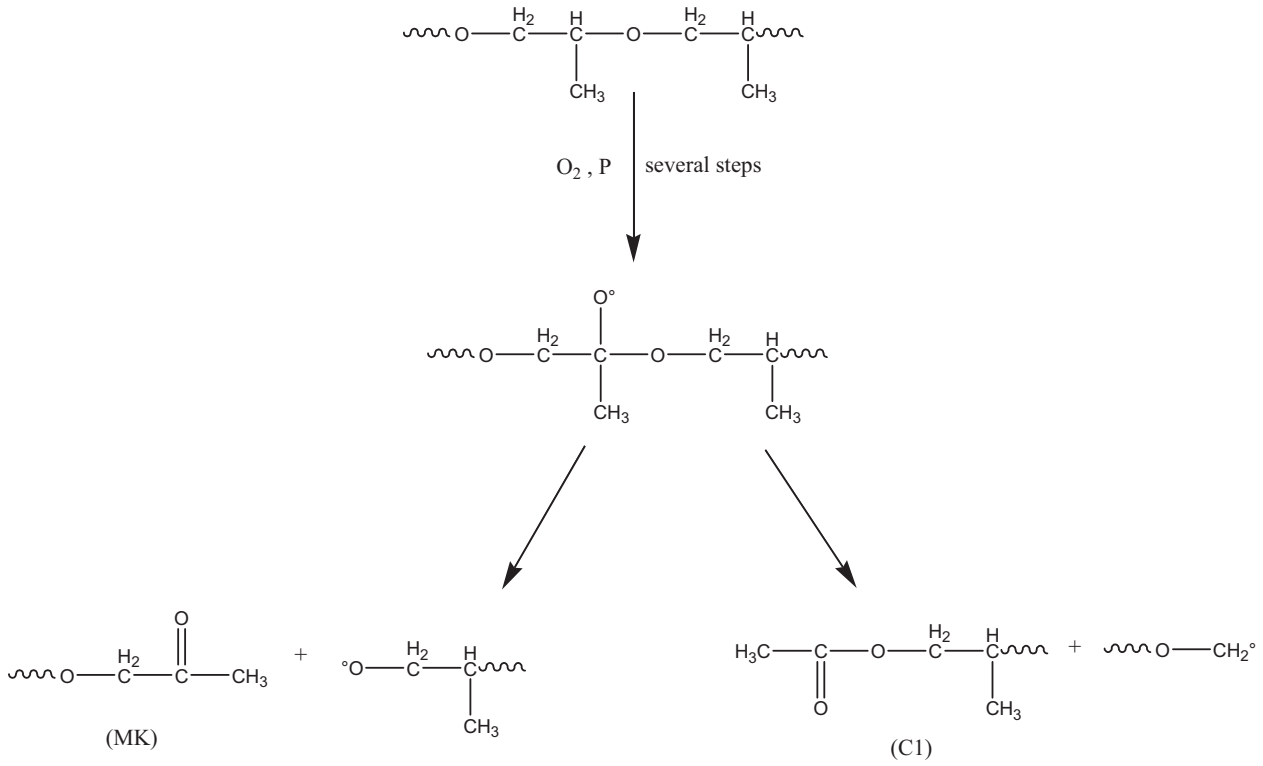

Fig. 7. Possible route for acetate formation in POPA networks.

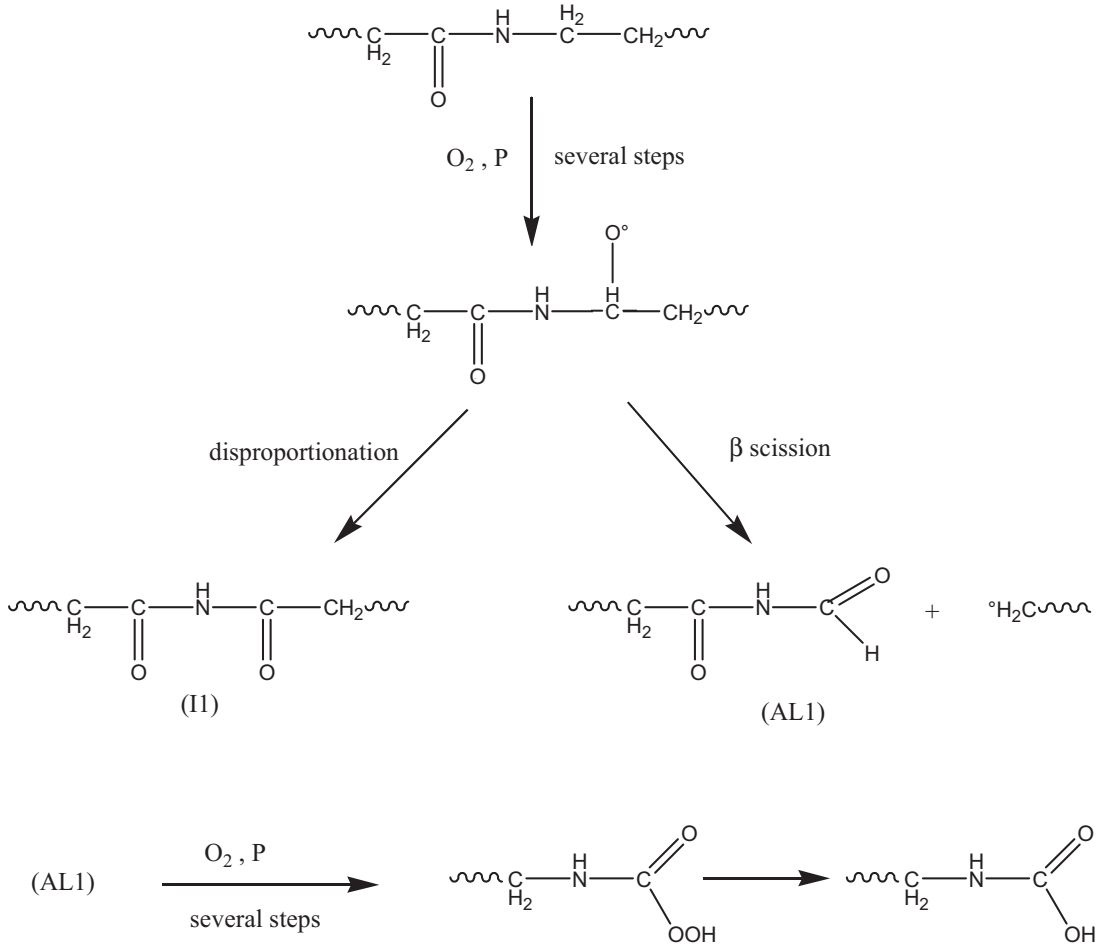

Fig. 8. Oxidation of PAA segments.

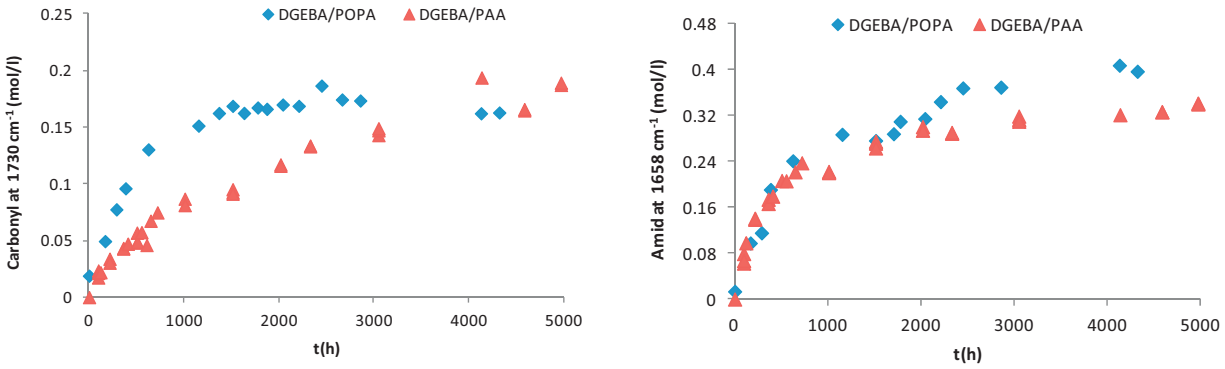

Fig. 9. Carbonyl (left) and amides (right) build-up at 110 °C for DGEBA/POPA (♦) and DGEBA/PAA(▲).

Table 1
Initial rates values (mol L^{-1} s^{-1}) of carbonyl and amides formation for both networks and their corresponded activation energies (E_a).

T(°C)	DGEBA/POPA		DGEBA/PAA	
	Carbonyl*10^{-9}(mol L^{-1} s^{-1})	Amide*10^{-9}(mol L^{-1} s^{-1})	Carbonyl*10^{-9}(mol L^{-1} s^{-1})	Amide*10^{-9}(mol L^{-1} s^{-1})
150	472	500	222	1060
130	–	361	83	306
110	56	111	25	167
90	28	28	14	56
70	19	17	5.6	25
E_a (kJ mol^{-1})	50.28 ± 3	56.22 ± 2	57.17 ± 0.8	55.2 ± 0.9

are almost equal. Amide build-up is faster in PAA networks than in POPA ones, the reverse is true for carbonyl build-up.

The fact that kinetics does not display induction periods and the low values of activation energies can be interpreted as consequences of the very low stability of hydroperoxydes. This is a common feature of polymers containing heteroatom such as O and N in α position of the reactive site (polyamides [24–26], polyether [27,28]).

According to Table 1, initial rates values, as well as activation energies, are close in both systems when it comes to amid formation. Taking into consideration this information and the fact that amides are formed at higher rate than carbonyls in both systems could be explained as follows: the most important initiating species in both networks: the α amino hydroperoxide is almost identical. Its decomposition determines, for a great part, the whole activation energy. Peroxy radicals which are the chain carriers of oxidation, propagate partly by attack of the diamine segment, partly by attack of the DGEBA segment. Chain transfer is obviously easier on POPA segments than on PAA ones which leads to higher concentration of carbonyls in the beginning of exposure in case of POPA (as shown in Fig. 9 left).

Concerning the behavior at long term, the following observations can be made:

In the case of carbonyls, the existence of horizontal asymptote, indicating equilibrium or a saturation phase, can be suspected in some cases (Fig. 9 left) but it is not systematically observed.

In the case of amides in contrast, Fig. 10 allows to understand the nature of the auto-retarded process.

Also in Fig. 10, related to amide growth in PAA samples, one can observe that at $T = 110$ °C, the curve displays a pseudo-asymptote or rather a widely spread maximum. However, at $T = 150$ °C where there is a clear maximum, the amide concentration decreases slowly after about 300 h.

The simplest explanation suggests the following: for a given network node, when a α amino methylene is attacked, the tertiary amine is transformed into tertiary amide. The second methylene is eventually less reactive but it can also undergo oxidation, transforming for instance the tertiary amide into imide which doesn't

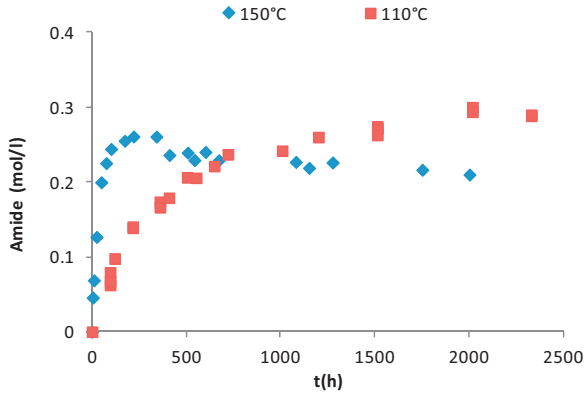

Fig. 10. Amide build-up in PAA films at 110 (■) and 150 °C (♦).

display absorption band in the 1650 ± 30 cm^{-1} region. The curves are thus expected to have the shape of Fig. 11 in which the timescale is not specified and depends on temperature.

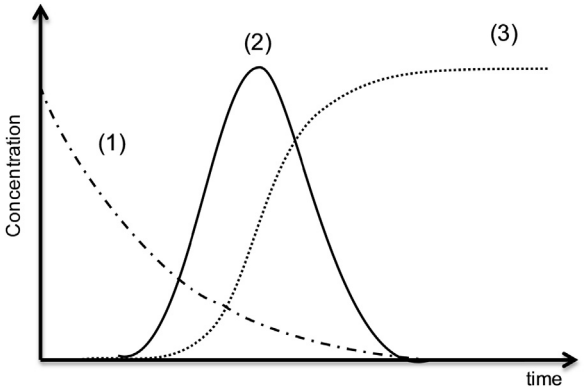

Fig. 11. Presumed shape of the kinetic master curves of relative concentrations of (1) reactive methylene; (2) amides; (3) imides or other secondary products.

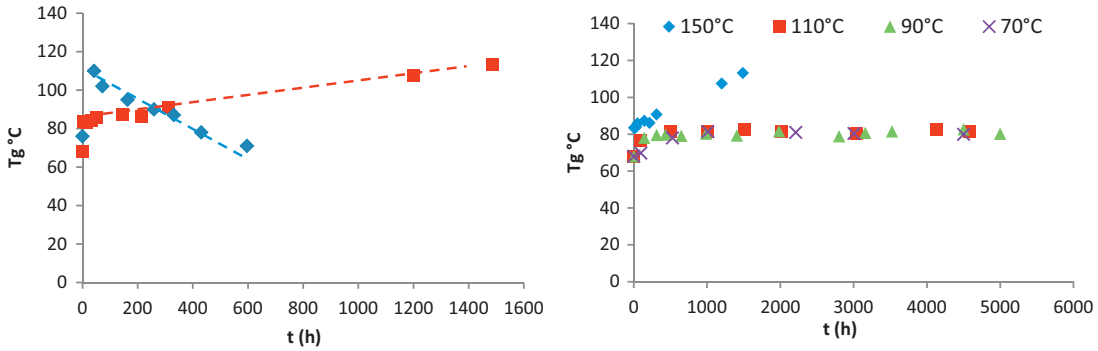

Fig. 12. (Left) T_g values for DGEBA/POPA (♦) and DGEBA/PAA (■) after exposure in air at 150 °C. (Right) T_g values of DGEBA/PAA after exposure under several temperatures.

3.6. Glass transition temperature

In both systems, the glass transition temperature T_g increases rapidly in the first hours of exposure to reach a value of 10–30 °C higher than initial one. This increase is obviously due to post-cure; it stops when the reactive groups have been almost totally consumed. After this initial period of a few days duration, slow changes attributed to thermal aging are observed (Fig. 12).

For DGEBA/POPA networks, T_g reaches a maximum after a time ranging from 70 h at 150 °C to 1500 h at 90 °C and then decreases at a rate that is an increasing function of temperature;

For DGEBA/PAA networks, in contrast, after the previously seen post-cure initial episode, T_g remains almost constant (at $T \leq 110$ °C) or increases (at 150 °C).

It appears thus that chain scission (of which the consequence is a decrease of the cross-link density) predominates at long term in DGEBA/POPA systems whereas cross-linking predominates at long term in DGEBA/PAA systems at high temperature.

3.7. Sol–gel analysis

The soluble fraction has been plotted against exposure time in Fig. 13. It increases, eventually after a pseudo-induction time, in all the cases revealing the existence of chain scissions. This increase is more important in DGEBA/POPA networks (maximum ~23%) than in DGEBA/PAA networks (maximum ~5–6%). This behavior is consistent with T_g data since degradation (chain scission) effects are observed only on DGEBA/POPA. The fact that the soluble fraction increases in DGEBA/PAA indicates the existence of some degradation coexisting with cross-linking in the system.

As it has been shown, there is a lot of oxidation processes able to induce chain scission. On the other hand, oxidative cross-linking processes are scarcer.

In the absence of double bonds and under oxygen excess, we can only imagine a termination process leading to a peroxide bridge:

$$POO^{\circ} + POO^{\circ} \rightarrow P{-}O{-}O{-}O{-}O{-}P$$

$$P{-}O{-}O{-}O{-}O{-}P \rightarrow [PO^{\circ}\ PO^{\circ}]_{cage} + O_2$$

$$[PO^{\circ}\ PO^{\circ}]_{cage} \rightarrow P{-}O{-}O{-}P(\text{cross-link})$$

$$[PO^{\circ}\ PO^{\circ}]_{cage} \rightarrow P{-}OH + P{=}O(\text{disproportionation})$$

$$[PO^{\circ}\ PO^{\circ}]_{cage} \rightarrow 2PO^{\circ} \rightarrow \text{reactionamongwhichchainscissions}$$

Cage combination of PO° radicals to give a peroxide bridge is in competition with disproportionation and escape from the cage. Disproportionation is favored when POO° and PO° are secondary radicals. The escape from the cage is expected to be favored by an increase of mobility.

There is however another possible case of cross-linking: when oxygen is not in excess, alkyl radicals can participate to termination, especially by coupling reactions:

$$P^{\circ} + POO^{\circ} \rightarrow P{-}O{-}O{-}P$$

$$P^{\circ} + P^{\circ} \rightarrow P{-}P$$

In POPA segments, coupling of tertiary radicals P° could be disfavored by steric hindrance, in contrast in PAA segments, coupling of P° radicals must be favored at low temperature. The current experimental data do not permit to establish if oxygen is or not in excess. However, cases where oxygen is in excess at atmospheric pressure are very scarce [29]. It can be thus reasonably supposed that cross-linking which is disfavored in DGEBA/POPA, results in DGEBA/PAA

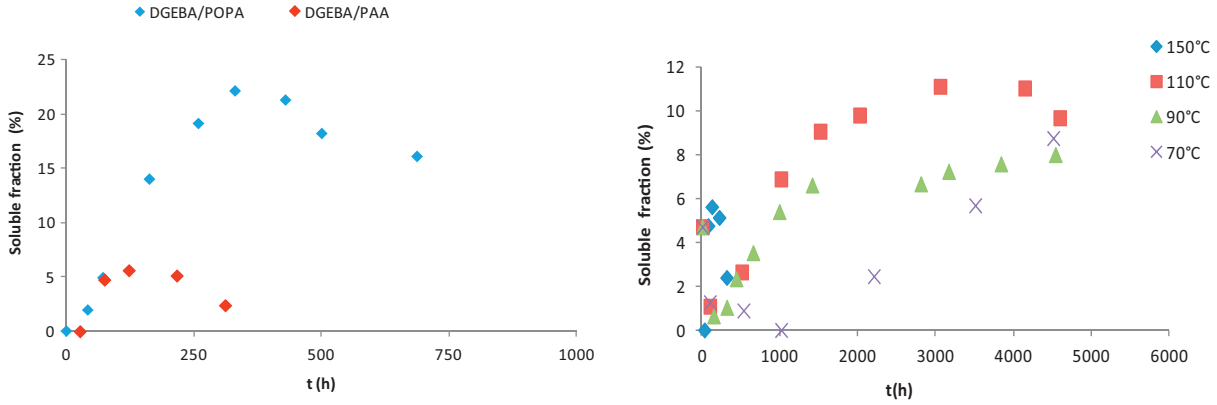

Fig. 13. (Left) Comparaison of soluble fraction values for DGEBA/POPA (♦) and DGEBA/PAA (♦) under thermal exposure at 150 °C. (Right) Soluble fraction values of DGEBA/PAA system under 70 (X), 90 (▲), 110 (■) and 150 °C (♦).

from radical coupling involving probably P° radicals. In these latter samples, cross-linking coexists with chain scission.

4. Conclusions

The thermal aging of epoxy networks based on DGEBA and hardened by POPA or PAA diamines has been studied in air at temperatures ranging from 70 to 150 °C by IR, DSC and sol–gel analysis. The results can be summarized as follows:

In both systems, amides appear as the major oxidation products showing that an important part of oxidation events occurs in the immediate vicinity of tertiary amines related to network nodes.

Polyamide segments of PAA are less reactive than polyoxypropylene ones of POPA owing to the existence, in these latter, of highly labile tertiary CH bonds. The radical attack of these sites leads to methyl ketone and, possibly, to formate formation.

Occurrence of post-cure, in the early period of exposure and heterogeneity, linked to eventual control of oxidation kinetics by oxygen diffusion, make difficult the quantitative analysis of chain scission and cross-linking processes. However, it can be observed that chain scission tends to predominate in POPA networks whereas cross-linking tends to predominate in PAA networks. This is an important observation from a practical point of view because chain scission and cross-linking have not the same consequences on mechanical (especially fracture) properties.

References

[1] N. Khelidj, X. Colin, L. Audouin, J. Verdu, Nucl. Instrum. Methods Phys. Res. B 236 (2005) 88–94.
[2] F. Djouani, Y. Zahra, B. Fayolle, M. Kuntz, J. Verdu, Radiat. Phys. Chem. 2 (2012) 54–62.
[3] T. Dyakonov, P.J. Mann, Y. Chen, W.T.K. Stevenson, Polym. Degrad. Stab. 54 (1996) 67–74.
[4] J. Pospisil, Z. Horak, Z. Krulis, S. Nespurek, S. Kuroda, Polym. Degrad. Stab. 65 (1999) 405–414.
[5] H.M. Le Huy, V. Bellenger, M. Paris, J. Verdu. Polym. Degrad. Stab. 35 (1992) 171–179.
[6] T. Dyakonov, P.J. Mann, Y. Chen, T.K. Stevenson, Polym. Degrad. Stab. 54 (1996) 67–83.
[7] P. Jain, V. Choudhary, I.K. Varma, Eur. Polym. J. 39 (2003) 181–187.
[8] I.D. Maxwell, R.A. Pethrick, Polym. Degrad. Stab. 5 (1983) 275–301.
[9] L. Barral, J. Cano, J. Lopez, I. Lopez-Bueno, P. Nogueira, M.J. Abad, J. Therm. Anal. Calorim. 60 (2000) 391–399.
[10] P. Musto, G. Ragosta, P. Russo, L. Mascia, Macromol. Chem. Phys. 202 (2001) 3445–3458.
[11] F. Delor-Jestin, D. Drouin, P.Y. Cheval, J. Lacoste. Polym. Degrad. Stab. 91 (2006) 1247–1255.
[12] F.P.J. Awaja, Pigram. Polym. Degrad. Stab. 94 (2009) 651–658.
[13] A. Cherdoud-Chihani, M. Mouzali, M. J. M. Abadie J. Appl. Polym. Sci 69 (1998) 1167–1178.
[14] L. Barral, J. Cano, A.J. Lopez, J. Lopez, P. Nogueira, C. Ramirez, Thermochim. Acta 269 (1995) 253–259.
[15] B. Mailhot, S. Morlat-Therias, M. Ouahioune, J.L. Gardette, Macromol. Chem. Phys. 206 (2005) 575–584.
[16] S.G. Hong, Polym. Degrad. Stab. 48 (1995) 211–218.
[17] J. Decelle, N. Huet, V. Bellenger, Polym. Degrad. Stab. 81 (2003) 239–248.
[18] J.S. Chen, Polymer 45 (2004) 1939–1950.
[19] X. Buch, M.E.R. Shanahan, Polym. Degrad. Stab. 68 (2000) 403–411.
[20] J. Verdu, Oxidation Aging or Polymers, iSTE-Wileye, 2012, pp. 238.
[21] V. Bellenger, J. Verdu, Polymer Commun. (1986) 27.
[22] P. Nordling, T.L. Lee, A.V. Tobolsky, Rubber Chem. Technol. 38 (1965) 1198–1205.
[23] V. Bellenger, J. Verdu, J. Appl. Polym. Sci. 30 (1985) 363–374.
[24] G. Subiman, D. Khastgir, A.K. Bhowmick, P.G. Mukunda, Polym. Degrad. Stab. 67 (2000) 427–436.
[25] W. Dong, P. Gijsman, Polym. Degrad. Stab. 95 (2010) 1054–1062.
[26] E. Richaud, O. Okamba Diogo, B. Fayolle, J. Verdu, J. Guilment, F. Fernagut, Polym. Degrad. Stab. 98 (2013) 1929–1939.
[27] B. Fayolle, J. Verdu, M. Bastard, D. Piccoz, J. Appl. Polym. Sci. 107 (2008) 1783–1792.
[28] J.D. Cooney, D.M. Wiles, J. Anal. Appl. Pyrolysis 18 (1990) 163–173.
[29] J. Verdu, Oxidation Aging of Polymers, iSTE-Wiley, 2012.